Compressive Sensing and Sparse Signal Processing Methods for Direction of Arrival Estimation (DOA) with MIMO Radar

Emre Ertin
205 Dreese Lab 2015 Neil Avenue Columbus, OH 43035
UNITED STATES

ertin.1@osu.edu

ABSTRACT

Direction finding has roots dating back to the introduction of the wireless communication technology, with first algorithms appearing in the literature early in the twentieth century. Motivated by the widespread adoption of Multi-Input Multi-output (MIMO) architectures in wireless communication systems, radar systems which can transmit independent waveforms on multiple antennas coupled with independently sampled receive arrays have been suggested for improving detection, parameter estimation and clutter suppression capabilities. In this paper we present a compressive radar architecture that combines multitone linear frequency modulated (LFM) waveforms on transmit with classical stretch processor and sub-Nyquist sampling on receive. The proposed compressive illumination scheme has fewer random elements than previously proposed compressive radar designs based on stochastic waveforms, resulting in reduced storage and complexity for implementation. Recovery guarantees for the proposed compressive illumination scheme is presented for the joint estimation of range and DOA. Finally, simulation results are presented to study recovery performance as a function of system parameters for targets both on and off the grid.

1.0 INTRODUCTION

Direction finding has roots dating back to the introduction of the wireless communication technology, with first algorithms appearing in the literature early in the twentieth century. As the radio frequency technology shifted from analog to digital, detection and tracking a large number of emitters become a possibility using an array of antennas sampled and processed in digital domain. Motivated by the widespread adoption of Multi-Input Multi-output (MIMO) architectures in wireless communication systems, radar systems which can transmit independent waveforms on multiple antennas coupled with independently sampled receive arrays have been suggested for improving detection, parameter estimation and clutter suppression capabilities. energy from multiple pulses and multiple antenna elements can be processed jointly to solve a multitude of inference tasks including detection, tracking and classification [1]. In the following we focus primarily on the problem of estimation of Direction of arrival (DOA), however we note that in radar systems the DOA problem is often coupled with range and Doppler frequency estimation and detection.

In this paper, we focus on coherent MIMO radar systems with closely separated antennas, such that the angle of arrival of each scatterer in the illuminated scene is approximately the same for all phase centers. The distinct advantage of a multi-antenna radar system with independent transmit waveforms is the increased number of degrees of freedom leading to improved resolution~ detection~, and parameter estimation performance. Additionally, MIMO radar systems with multiple transmit and receive elements employing independent waveforms on transmit can provide spatial processing gains by exploiting the diversity of channels between targets and radar [2, 3]. In the following, we formulate the direction of arrival estimation problem in the context of MIMO radar, describe traditional DOA estimation methods and briefly review known results on performance limits. In Section 2, we present a compressive radar architecture that combines multitone linear frequency modulated (LFM) waveforms on transmit with classical stretch processor [5] and sub-Nyquist sampling on receive. The proposed compressive illumination scheme has fewer random elements than previously proposed compressive radar designs based on stochastic waveforms,

resulting in reduced storage and complexity for implementation. Recovery guarantees for the proposed compressive illumination scheme is presented for the joint estimation of range and DOA. We present bounds on the operator norm and mutual coherence of the structured sensing matrix representing the proposed scheme and show that for sufficiently large number of modulating tones, high resolution recovery is guaranteed for a sparse scene using sampling rates that scale linearly with the scene sparsity. Finally, simulation results are presented to study recovery performance as a function of system parameters for targets both on and off the grid.

2.0 CS MODELS AND SPARSE SIGNAL METHODS FOR DOA

2.1 Overview

Compressive MIMO radar architectures purposefully subsample the signal in time and spatial domain to reduce the load on the signal acquisition system and operate at sampling speeds not available currently [4]. As a result, straightforward match filtering results in strong range/angle sidelobes, rendering traditional beamformer methods suboptimal. In contrast, sparse reconstruction algorithms can successfully detect and localize targets by imposing sparse priors on the number of targets in the scene.

In the following we will study in detail the estimation problem of range and angle of arrival of targets using a specific MIMO radar architecture employing compressive illumination transmit waveforms [33, 34] and review theoretical results reported in [39, 40, 37]. Many MIMO DOA processing chains use a sequential strategy where detection in range is followed by detection in angle of arrival. This strategy is optimal only if there is perfect orthogonality between the transmit signals, as in the case of time division multiple access (TDMA) where only one transmitter is active at any time. For simultaneous transmit architectures, perfect orthogonality is unachievable between target returns for all delays and angles. Therefore, in the following we will pursue a joint estimation strategy for target range and DOA and characterize its performance using empirical and theoretical analysis. We will assume that the scene is comprised of a sparse set of dominant scattering centers. This assumption enables us to reduce the sampling rate at the receiver, thereby reducing the burden on acquisition systems. We present the uniform and non-uniform recovery guarantees for the proposed illumination framework and also conduct numerical simulations to illustrate the performance as a function of the system parameters.

2.2 Analytical Model for Compressive MIMO Sensor

We consider N_T transmitters and N_R collocated receivers that function as a MIMO radar system. This system employs the compressive illumination framework first proposed in [33] which is extended to the case of multiple transmitters and receivers for estimating the target range and angle of arrival in [39, 40]. The transmitter antenna elements are placed with a spacing of $d_T = 0.5$ and the receiver antenna elements are placed with a spacing of $d_R = 0.5N_T$ relative to the wavelength $\lambda_c = c/f_c$ of the carrier to obtain the virtual array with aperture length $N_T N_R$ m, where c is the velocity of light in vacuum, and f_c is the carrier frequency. The process used to generate the transmitted signal is shown in Figure 1.

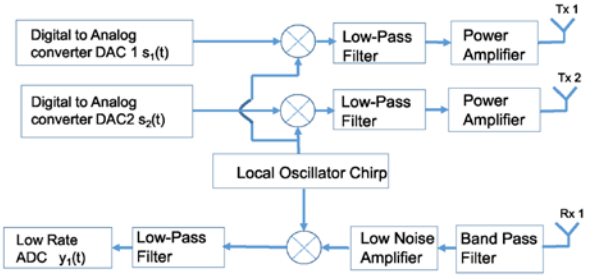

Figure 1: Block Diagram of the compressive transceiver

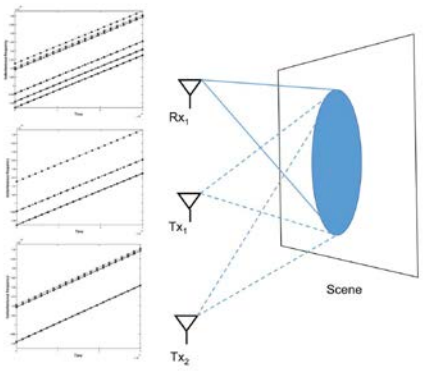

Figure 2: The time-frequency representations of the waveform employed by two transmitters Tx_1, Tx_2 and received signal at one of the collocated receiver Rx_1 are shown. The transmitted waveforms are obtained as a result of modulation of the linear frequency modulated waveform by a set of sinusoids with randomly chosen frequencies. The received signal is a weighted linear combination of the transmitted signals.

We discretize the frequency range $[0, B]$ into N frequencies $f_1, \cdots, f_N$, where $N = Bt_u$, t_u is the unambiguous time interval, and B is the system bandwidth. A subset of $N_c N_T$ tones are chosen at random from these N possible frequencies, where N_c is the number of modulating tones used in each transmitter. These chosen tones are used for modulating the LFM waveform with bandwidth $\beta \ll B$, using the Single Side-Band (*SSB*) modulation technique. We simplify this selection model for analysis by considering N independent indicator random variables $\hat{\gamma}_i \in \{0,1\}$ following a Bernoulli distribution with $P(\hat{\gamma}_i = 1) = N_c N_T / N$, and $P(\gamma_i = 0) = 1 - N_c N_T / N$ to select the tones that modulate the LFM waveform such that $N_c N_T$ waveforms are selected on an average. The chosen LFM waveforms are scaled by a sequence of independent and identical complex exponentials with uniformly distributed phases with the probability density function $f_\Phi(\phi_i) = 1/(2\pi), \phi_i \in [0, 2\pi]$. We define the sequence of random variables $\hat{c}_i$ that model this selection process as $\hat{c}_i = \hat{\gamma}_i \exp(j\Phi_i)$

Each selected waveform is assigned to one of the N_T transmitters at random with uniform probability. Let $\xi(i)$ be the discrete random variable that indicates the assignment of waveform i to transmitter l given by the uniform probability mass function $P(\xi(i) = l) = 1/N_T$, $l = 0, \cdots, N_T\text{-}1$, $i = 0, \cdots, N\text{-}1$. The transmitted signal from all the N_T transmitters can be written as

$$s(t) = \sum_{i=1}^{N} \hat{c}_i \frac{\exp\left(j2\pi\left[\hat{f}(i)t + \frac{\beta}{2\tau}t^2\right]\right)}{\sqrt{N_c N_T}} r\left(\frac{t - \frac{\tau}{2}}{\tau}\right)$$

where $r\left(\left(t - \frac{\tau}{2}\right)/\tau\right) = 1$ if $t \in (0, \tau)$ and 0 otherwise, and $\hat{f}(i) = f_c + f(i)$, for $i = 1, \cdots, N\text{-}1$. The instantaneous frequency of the transmitted and received modulated LFM signal as a function of time is illustrated in Figure 2. for the case of $N_T = 2, N_R = 1$.

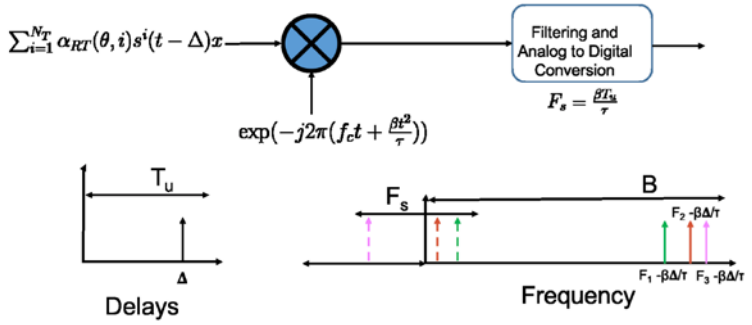

Figure 3: The figure illustrates the structure of the received signal due to a single scattering center located with range $c\Delta/2$ and angle θ. The stretch processing at the receiver utilizes the transmitted LFM waveform before the modulation step. The effect of this operation recovers the modulating tones, shown in solid lines in the frequency domain, which are further modulated by a complex exponential with a frequency that depends on the range of the scattering center. The sampling rate is set as $F_s = \beta\tau/t_u$, which leads to an aliased spectrum shown in dashed lines.

Figure 3 shows the stretch processing operation implemented at a particular receiver. The sampling rate at the receiver after stretch processing is $F_s = \beta t_u/\tau$, which leads to $M = \beta t_u$ samples at stretch processor output at each receiver. Since the sampling rate is much lower than the Nyquist rate required for the modulating tones, the multi-tone spectrum corresponding to a target with a delay of Δ aliases to the range $[-F_s/2, F_s/2]$. Unlike the problem of determining spectral content from uniform time samples [31,32], it is established that we can uniquely recover the delay and angle of arrival of a sparse set of targets given a sufficient number of modulating tones are used in the illumination scheme. The n^{th} sample $y_k(n)$ at the stretch processor at receiver k due to a target located at a delay $\Delta \in [0, t_u]$ and an angle of arrival $\theta \in [0, 2\pi]$ with amplitude $x \in \mathbb{C}$ is given by

$$y_k(n) = \sum_{i=1}^{i=N} \hat{c}_i \exp(-j2\pi f(i)\Delta)\alpha_R(\theta;k)\frac{\alpha_T(\theta;\xi(i))x}{\sqrt{N_T N_R N_c M}} \exp\left(j2\pi\left(f(i)-\frac{\beta\Delta}{\tau}\right)\frac{n}{F_s}\right) + w_{k,n},$$

$$y_k(n) = \Psi_{k,n}(\Delta,\theta) + w_{k,n},$$

$$\Psi_{k,n}(\Delta,\theta) = \sum_{i=1}^{i=N} \hat{c}_i \exp(-j2\pi f(i)\Delta)\alpha_R(\theta;k)\frac{\alpha_T(\theta;\xi(i))x}{\sqrt{N_T N_R N_c M}} \exp\left(j2\pi\left(f(i)-\frac{\beta\Delta}{\tau}\right)\frac{n}{F_s}\right),$$

$$\text{where } \Psi(\Delta,\theta) = \left[\Psi_{1,1}(\Delta,\theta),\cdots,\Psi_{1,M}(\Delta,\theta),\cdots,\Psi_{N_R,M}(\Delta,\theta)\right]^T,$$

$w_{k,n}$ is the n^{th} noise sample at receiver k, $\alpha_R(\theta;k) = \exp(j2\pi d_R(k)\theta)$ is the array steering parameter corresponding to receiver k, $\alpha_T(\theta;\xi(i)) = \exp(2j\pi d_T\xi(i)\theta)$ is the steering parameter corresponding to the chosen transmitter specified by the random variable $\xi(i)$ for the i^{th} waveform, $\Psi(\Delta,\theta) \in \mathbb{C}^{N_R M}$ and represents the signal component due to a target located at range Δ and angle of arrival θ referred to as an atom. We further discretize the range and angle of arrival space. The unambiguous interval from $[0, t_u]$ is discretized at a resolution of $1/B$ corresponding to the resolution achieved by a system employing a signal of bandwidth B resulting in $N = Bt_u$ bins. Each delay bin is denoted as $\Delta_m = m/B, m = 0,1,\cdots,N\text{-}1$.

The angle of arrival characterized by $\sin\theta \in [-1,1]$ is partitioned into $N_\theta = N_T N_R$ grids. Each angle bin is denoted as $\theta_v \in \{2v/(N_T N_R) | v = -N_T N_R/2, \cdots, N_T N_R/2 - 1\}$. The receiver and transmitter steering vectors as function of the angle of arrival θ_v are defined as

$$\boldsymbol{\alpha}_{\mathbf{R}}(\theta_v) = \left[1 \quad \cdots \quad \exp\left(j\bar{d}_R(N_R-1)\theta_v\right)\right]^T, \text{and}$$
$$\boldsymbol{\alpha}_{\mathbf{T}}(\theta_v) = \left[1 \quad \cdots \quad \exp\left(j\bar{d}_T(N_T-1)\theta_v\right)\right]^T,$$

respectively, where $\bar{d}_R = 2\pi d_R$ and $\bar{d}_T = 2\pi d_T$. The normalized samples at the stretch processor output $y_k(n)$ at receiver k due to the targets in the region of interest is given by

$$y_k(n) = \sum_{v=0}^{N_T N_R - 1} \sum_{\substack{m=0 \\ i=1}}^{\substack{m=N-1 \\ i=N}} \hat{c}_i\, \alpha_R(\theta_v; k) \frac{\alpha_T(\theta_v; \xi(i)) x(v,m)}{\sqrt{N_T N_R N_c M}} \exp(-j2\pi f(i)\Delta_m) \exp\left(\frac{j2\pi n}{F_s}\left(f(i) - \frac{\beta\Delta_m}{\tau}\right)\right) + w_{k,n},$$

where $k = 1, \cdots, N_R$, $n = 0, \cdots M\text{-}1$, and $x_{v,m} \in \mathbb{C}$ is the scattering coefficient at range bin m and angle of arrival bin v. The concatenated output from all the N_R receivers can be compactly written as $\mathbf{y} = \mathcal{A}\mathbf{x} + \mathbf{w}$.

$$\mathbf{y} = \left[\mathbf{y}_1 \cdots \mathbf{y}_{N_R}\right]^T, \mathbf{y}_k = \left[y_k(0) \cdots y_k(M-1)\right]^T \in \mathbb{C}^M$$
$$\mathbf{w} = \left[\mathbf{w}_1 \cdots \mathbf{w}_{N_R}\right]^T, \mathbf{w}_k = \left[w_{k,0} \cdots w_{k,M-1}\right]^T \in \mathbb{C}^M$$

where the signal is given by

is the zero mean additive noise following a Complex Gaussian distribution with variance σ^2, and $\mathbf{x} \in \mathbb{C}^{N N_T N_R}$ contains the complex scattering amplitudes associated with targets at all possible grid locations in the range-angle domain. The sensing matrix $\mathcal{A} \in \mathbb{C}^{N_R M \times N_\theta N}$ can be expressed as a series of deterministic matrices with random coefficients as follows

$$\mathcal{A} = \sum_{i=1}^{N} \hat{c}_i \left(\bar{\boldsymbol{\alpha}}_{\mathbf{R}} \bar{\boldsymbol{\alpha}}_{\mathbf{T}}(\boldsymbol{\xi}(\mathbf{i}))\right) \otimes \left(\mathbf{H}_i \bar{\mathbf{A}} \mathbf{D}_i\right),$$

$$\text{where, } \bar{\boldsymbol{\alpha}}_{\mathbf{R}} = \sqrt{\frac{1}{N_R N_T}} \left[\boldsymbol{\alpha}_{\mathbf{R}}(\theta_0) \quad \cdots \quad \boldsymbol{\alpha}_{\mathbf{R}}(\theta_{N_\theta - 1})\right]$$
$$\bar{\boldsymbol{\alpha}}_{\mathbf{T}}(\boldsymbol{\xi}(\mathbf{i})) = \text{diag}\left(\exp\left(j\bar{d}_T \xi(i)\theta_0\right) \cdots \exp\left(j\bar{d}_T \xi(i)\theta_{N_\theta - 1}\right)\right)$$

where $i = 0, \cdots, N\text{-}1$ and $r = 0, \cdots, N\text{-}1$. $\bar{\boldsymbol{\alpha}}_{\mathbf{R}} \in \mathbb{C}^{\mathbf{N_R} \times \mathbf{N_\theta}}$ is the matrix consisting of receiver steering vectors for all the bins of angle of arrival, $\otimes$ represents the Kronecker product and $\bar{\boldsymbol{\alpha}}_{\mathbf{T}}(\boldsymbol{\xi}(\mathbf{i})) \in \mathbb{C}^{N_\theta \times N_\theta}$ is the random diagonal matrix with diagonal elements as the randomly chosen transmitter's component of the steering vector for all the angle bins. The individual components are as follows

$$\bar{\mathbf{A}} = \frac{1}{\sqrt{M N_c}} \left[\bar{\mathbf{A}}(0) \quad \cdots \quad \bar{\mathbf{A}}(N-1)\right]$$
$$\bar{\mathbf{A}}(r) = \left[1 \quad \exp\left(-2\pi j \frac{r}{N}\right) \quad \cdots \quad \exp\left(-2\pi j \frac{r(M-1)}{N}\right)\right]^T,$$
$$\mathbf{D}_i = \text{diag}\left[1 \quad \exp\left(-j2\pi \frac{i}{N}\right) \quad \cdots \quad \exp\left(-j2\pi \frac{i(N-1)}{N}\right)\right],$$
$$\mathbf{H}_i = \text{diag}\left[1 \quad \exp\left(j2\pi \frac{ip}{M}\right) \quad \cdots \quad \exp\left(j2\pi \frac{ip(M-1)}{M}\right)\right],$$

where $i = 0, \cdots, N\text{-}1$ and $r = 0, \cdots, N\text{-}1$, $\bar{\mathbf{A}} \in \mathbb{C}^{M \times N}$ are the samples from tones that correspond to each delay bin generated as a result of the de-chirping process in case of a single chirp system, $\mathbf{H}_i \in \mathbb{C}^{M \times M}$ is the shift in frequency due to the i^{th} modulating tone, and $\mathbf{D}_i \in \mathbb{C}^{N \times N}$ is the phase term associated with different delay bins due to the i^{th} modulating tone.

Each column of the sensing matrix $\mathcal{A}$ can be written as $\mathcal{A}(m,v) = \left(\boldsymbol{\alpha}_{\mathbf{R}}(\boldsymbol{\theta}_{\mathbf{v}}) \otimes (\mathbf{E}_{\mathbf{m}}\mathbf{F}\mathbf{G}_{\mathbf{m}})\right)\hat{\mathbf{c}}(v)$ $\hat{c}_r(v) = \hat{c}_r\,\alpha_T(\theta_v;\xi(r))$

where $m,r = 0,\cdots,N\text{-}1$, $v = 0,\cdots,N_\theta\text{-}1$. $\hat{\mathbf{c}}(s) = [\hat{c}_0(s)\cdots\hat{c}_{N-1}(s)]^T \in \mathbb{C}^N$ is the random vector with independent components expressed as a product of 2 random variables: a variable that selects the chirp waveform, and an independent variable that allocates the waveform to a particular transmitter.

2.3 Theoretical Recovery Guarantees for Targets on grid

We consider a statistical model studied in [19] for the sparse range profile of targets. We assume that the targets are located at the $NN_\theta = NN_RN_T$ discrete locations corresponding to different delay bins and angle bins. For the case of single transmitter and receiver case, this reduces to N delay bins. The support of the K-sparse range profile is chosen uniformly from all possible subsets of size K. The complex amplitude of non-zero components is assumed to have an arbitrary magnitude and uniformly distributed phase in $[0,2\pi]$. We show that the measurement model presented in the previous section satisfies the conditions on mutual coherence given in [36] and also provide a bound on the sparsity level of range profile, which guarantees successful support recovery of almost all sparse signals using LASSO with high probability from noisy measurements. The following theorems (for proofs please see reference [39,37]) provide the recovery guarantee for a compressive MIMO radar system.

Non-uniform Recovery Guarantee for Random Support Sets: Consider a compressive MIMO radar system with the measurement model $\mathbf{y} = \mathcal{A}\mathbf{x} + \mathbf{w}$, where $\mathcal{A} \in \mathbb{C}^{N_RM\times N_RN_TN}$ is defined in Section 1.5.2 such that the target scene $\mathbf{x}$ is drawn from a K-sparse model with complex unknown amplitudes and observed in i.i.d. noise process $\mathbf{w} \sim \mathcal{CN}(0,\sigma^2 I)$. The support of the targets in the scene can be recovered using a LASSO estimator with high probability for a system using M samples at each receiver, N_c tones at each transmitter with $M \sim \mathcal{O}(\log^3(NN_RN_T))$ and $N_c \sim \mathcal{O}(N/N_T)$, if the target scene consists of K targets with

$K \sim \mathcal{O}\left(\frac{N_RM}{\log^2(NN_RN_T)}\right)$ of minimum amplitude $\min_{k\in\mathbf{S}}|x_k| > \frac{8}{\sqrt{1-\epsilon}}\sigma\sqrt{2\log(NN_RN_T)}$

We note that the number of measurements (N_RM) depends linearly on the number of targets (K) but only logarithmically on the size of the search space of (NN_RN_T) angle-range bins.

2.4 Simulation Study of Off-grid Recovery

We consider the MIMO system with N_T transmitters and N_R receivers with M measurements per receiver. The samples at the stretch processor's output at receiver k due to a target with a time of arrival given by Δ and angle of arrival θ as given before. For a scene containing K scattering centers, the measurements are given by

$$\begin{aligned}\mathbf{y} &= \sum_{k=1}^{K} x_k\,\boldsymbol{\Psi}(\Delta_k,\theta_k) + \mathbf{w},\\ &= \sum_{k=1}^{K} x_k \int_{\Delta,\theta} \boldsymbol{\Psi}(\Delta,\theta)\delta(\Delta\text{-}\Delta_k,\theta\text{-}\theta_k)\,d\Delta d\theta + \mathbf{w}\\ &= \int_{\Delta,\theta} \boldsymbol{\Psi}(\Delta,\theta)\,d\nu(\Delta,\theta) + \mathbf{w},\end{aligned}$$

where $\mathbf{w} \sim \mathcal{CN}(0,\sigma_n^2\mathbf{I}) \in \mathbb{C}^{N_RM}$ is the receiver noise following

a zero-mean complex Gaussian distribution with variance σ_n^2, x_k are the complex scattering coefficients, Δ_k, θ_k are the delay and angle of arrival for each scattering center, δ is the Dirac delta generalized function, and $\nu = \sum_k x_k \, \delta(\Delta\text{-}\Delta_k, \theta\text{-}\theta_k)$ is the discrete measure with complex coefficients. $\boldsymbol{\Psi} \in \mathbb{C}^{N_R M}$ is the known structured response parametrized by the time and angle of arrival of the scattering center due to the proposed illumination scheme. The space of unknown parameters is usually discretized, and the non-linear estimation problem is converted to a linear inverse problem. In the previous chapter, we established that the operator representing our system is well-conditioned for a sparse scene provided we have sufficient samples and modulating tones. In this sequel, we solve the following problem in the continuum

$$\left\| \mathbf{y} - \int_{\Delta,\theta} \boldsymbol{\Psi}(\Delta,\theta) d\nu(\Delta,\theta) \right\|_2^2 \quad \text{Subject to} \|\nu\|_{TV} \leq \tau,$$

where $\mathbf{y} \in \mathbb{C}^{N_R M}$ are the noisy measurements, ν is the discrete measure over the space of delay and angle of arrival, and $\|\nu\|_{TV}$ is the total-variation norm on the space of discrete measures with complex coefficients bounded by the problem specific parameter τ. The next section presents the details of the algorithm, which was proposed in [49] for solving the sparse linear inverse problem above.

2.5 Off-grid Recovery algorithm

Recently, multiple approaches have been suggested solving the off-grid target detection algorithms. Atomic norm formulation [53] of the problem leads to a closed form solution for frequency estimation problems [11]. Alternatively, one can obtain the solution by over-discretizing the search space into finer grids. It has been shown [50] that the ℓ_1 norm minimization in the over-discretized space converges to the atomic norm minimization in the continuum. The problem with this approach is that the computational complexity increases with the dimensionality of the parameter space. Instead of discretization, we apply the approach of [49] to exploit the fact that the measurement model is differentiable in the unknown parameters such as delay and angle of arrival of scattering centers to solve this off-grid problem.

Algorithm 1: Alternating descent conditional gradient method [49].

Data: Given $\mathbf{y}, \tau$, $\boldsymbol{\Psi}$, Ω, K_{max}, and $\nabla_{\theta \in \Omega} \boldsymbol{\Psi}$.
Result: Estimate complex weights $\mathbf{x}$, delay,angle of arrival of scattering centers $\{\boldsymbol{\theta}, \boldsymbol{\Delta}\} \in \Omega$.
Initialize k=1, support set $S = \{\emptyset\}$
While Convergence condition is not satisfied or $k \leq K_{max}$

Residual: $\mathbf{r}_k = \mathbf{y} - \sum_{i=1}^{k-1} \boldsymbol{\Psi}(\Delta_k, \theta_k) x_k,$

Gradient of loss function: $\mathbf{g}_k(\mathbf{r}_k) = \nabla_{\mathbf{r}}\left(0.5\|\mathbf{r}_k\|_2^2\right)$

$\{\Delta_k, \boldsymbol{\theta}_k\} = \arg\max_{\{\Delta,\theta\} \in \Omega} |\langle \Psi(\Delta,\theta), \mathbf{g}_k \rangle|,$

$S = S \cup \{\Delta_k, \boldsymbol{\theta}_k\}$

While

Compute weights: $\arg\min_{\|\mathbf{x}\|_1 \leq \tau} \|\boldsymbol{\Psi}_S \mathbf{x} - \mathbf{y}\|^2$

Prune Support: If $|x_k| = 0 \quad S = S \backslash \{\Delta_k, \theta_k\}$

Refine support: $S = S - \nabla_S \|\boldsymbol{\Psi}_S \mathbf{x} - \mathbf{y}\|^2$

end

$k = k + 1;$
end

Algorithm 1 provides the details of the alternating descent conditional gradient method used to solve the range, angle estimation problem with sparsity constraints. The method first selects the set of parameters in

the parameter space to fit the residual by the model at the current iterate, followed with a gradient update step where the weights and the support are refined. This non-convex problem of jointly estimating the weights and the parameters is solved by an alternating minimization approach. The weights are estimated by solving the finite dimensional problem on the detected support set by enforcing the ℓ_1 constraint on the weights. The support set is pruned such that only non-zero points in the support set are retained. Next, the support set is refined using the gradient information with the steepest descent method with line search.

2.6 Simulation Results

System parameters used in the numerical simulation is given in the table below. Signal to Noise ratio (SNR) of $15dB$ and under-sampling ratio of $M/N = 1/3$ is used in the simulations. We consider the number of transmitters $N_T = 16$, and the number of receivers $N_R = 4$ in our simulation. Each transmitter uses an LFM waveform modulated by $N_c = 2$ tones with a randomly chosen frequency shifts. We set the number of targets in the scene as $K = 100$ using the random support over the range-angle space. We compare the performance of the system as the number of modulating tones is varied using the metrics defined below. We define the set consisting of the true range of the scattering centers as $\mathcal{T} = \{r_i, \theta_i\} \subset \Omega$ with complex scattering coefficients $\{x_i\}$ for $i = 1, \cdots, K$, where K is the number of targets in the scene. We define N_i as the neighborhood of the true range r_i and angle of arrival θ_i, such that

$$N_i = \left\{(r,\theta): |r\text{-}r_i| \le \frac{0.2c}{(2B)} \text{ and } |sin(\theta)\text{-}\sin(\theta_i)| < \frac{0.4}{N_R N_T}\right\}$$

The region of false detections is defined as $\mathcal{F} = \Omega \backslash \{\cup_i N_i\}$

We consider the following performance measures to compare the systems employing different sets of modulating tones

- Total amplitude of false alarms:
$$m_1 = \sum_{(\hat{r}_i,\hat{\theta}_i)\in\mathcal{F}} |\hat{x}_i|.$$
- weighted direction of arrival localization error
$$m_2(\theta) = \sum_{(\hat{r}_i,\hat{\theta}_i)\in\cup_j N_j} |\hat{x}_i| \min_{(r,\theta)\in\mathcal{T}} \left\|\sin(\hat{\theta}_i)\text{-}\sin(\theta)\right\|^2.$$
- weighted range localization error
$$m_2(r) = \sum_{(\hat{r}_i,\hat{\theta}_i)\in\cup_j N_j} |\hat{x}_i| \min_{(r,\theta)\in\mathcal{T}} \|\hat{r}_i\text{-}r\|^2.$$
- approximation error in the detected scattering coefficients
$$m_3 = \sum_{(r_i,\theta_i)\in\mathcal{T}} \left| x_j\text{-} \sum_{(r_l,\theta_l)\in N_i} \hat{x}_l \right|$$

We evaluate the performance profile of the two algorithms traditional beamforming and off-grid CS based sparse recovery. The performance profile tabulates fraction of the Monte Carlo simulations where one algorithm error was within β factor of the minimum error for that run. The performance profile is evaluated by repeating the experiment for different realizations of target denoted by the set $\mathcal{P}$. Analytically, the performance profile for the system parameter $s \in \mathcal{S}$, error metric m_i, and factor β, which specifies the ratio

$m_i(p,s)/\min_s m_i(p,s)$ is computed as follows $P_s(\eta;i) = \dfrac{\mathbf{card}\left\{p \in \mathcal{P}: m_i(p,s) \le \beta \min_s m_i(p,s)\right\}}{\mathbf{card}\{\mathcal{P}\}}$

To choose threshold for the traditional beamforming algorithm we computed the receiver operation curve for the two algorithms as given in Figure 4. For the off-grid sparse recovery algorithm we choose the operating point as probability of detection of 0.94 with a corresponding false alarm rate of $4x10^{-5}$. Then we choose the detection threshold for the beamformer output to achieve the same false alarm rate, which results in a significantly lower probability of detection rate of 0.38.

Figure 5 and 6 shows the performance profile of the two algorithms evaluated for all the error metrics computed using 100 target realizations. We observe that in each case CS based off-grid sparse recovery algorithm outperforms detections based on thresholding of the output of traditional delay-and sum Beamformer. Specifically, Figure 5 shows that, false alarm performance of CS sparse recovery was better than Beamformer detector in 96.5% of the Monte Carlo Runs. Beamformer false alarm performance was within 50% (β=1.5), of the best result in only 18% of the Monte Carlo runs. Figure 6 and 7 shows that, DOA and range localization error of CS sparse recovery was uniformly better than that of Beamformer. Finally, in Figure 8 we observe while the amplitude estimates of correctly detected targets of CS based algorithm are better than beamformer counterparts in 87% of the counterparts, the error performance of the two algorithms were competitive. The beamformer estimates were within 1.66 of the minimum error achieved in all of the simulation runs.

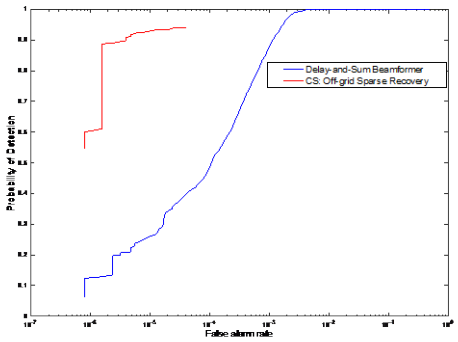

Figure 4: Receiver Operator Curve (ROC) for the two algorithms

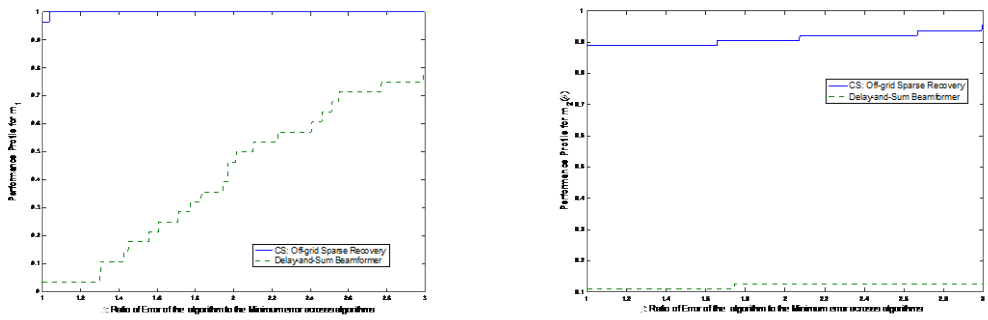

Figure 5a: Performance Profile of Beamformer and CS: off-grid sparse recovery algorithms comparing total amplitude of false alarm metric m_1. (b): Performance Profile of Beamformer and CS: off-grid sparse recovery algorithms comparing weighted direction of arrival localization error $m_2(\theta)$.

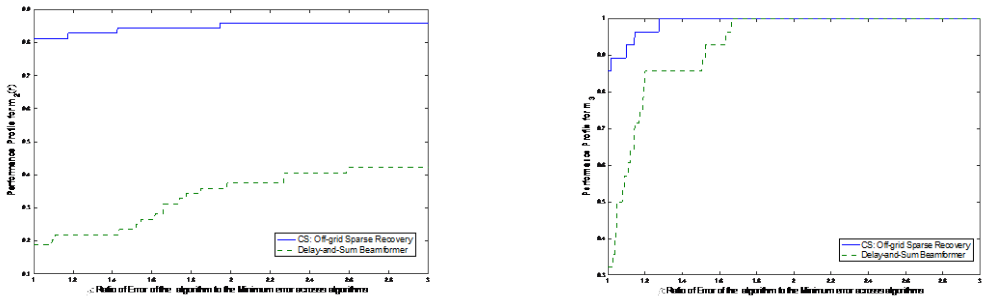

Figure 6 (a) Performance Profile of Beamformer and CS: off-grid sparse recovery algorithms comparing weighted range localization error $m_2(r)$. (b)Performance Profile of Beamformer and CS: off-grid sparse recovery algorithms comparing error in amplitude estimates of detected targets m_3.

2.7 Conclusion

Compressive MIMO radar architectures purposefully subsample the signal in time and spatial domain to reduce the load on the signal acquisition system. As a result, the received signal is subject to aliasing and match filtering results in strong range/angle sidelobes, rendering traditional processing methods suboptimal. Sparse reconstruction algorithms can successfully detect and localize targets for sparse target scenes through joint processing of the range/angle domain subject to sparsity constraints. Our theoretical analysis and simulation results show that compressive radar architectures paired with sparse reconstruction algorithms can outperform their traditional counterparts if the target scene is sufficiently sparse.

REFERENCES

[1] M. A. Richards, *Fundamentals of Radar Signal Processing*. New York, NY, USA: McGraw-Hill, 2014.

[2] P. Stoica and J. Li, *MIMO Radar Signal Processing*. Hoboken, NJ, USA: Wiley and Sons, 2008.

[3] S. Baskar and E. Ertin, "A software defined radar platform for waveform adaptive MIMO radar research," in *2015 IEEE Radar Conference (RadarCon)*, May 2015, pp. 1590–1594.

[4] R. H. Walden, "Analog-to-digital converter survey and analysis," *IEEE Journal on Selected Areas in Communications*, vol. 17, no. 4, pp. 539–500, Apr 1999.

[5] R. Middleton, "Dechirp-on-receive linearly frequency modulated radar as a matched-filter detector," *IEEE Transactions on Aerospace and Electronic Systems*, vol. 48, no. 3, pp. 2716–2718, July 2012.

[6] D. L. Donoho, "Compressed sensing," *IEEE Transactions on Information Theory*, vol. 52, no. 4, pp. 1289–1306, Apr. 2006.

[7] E. Candes, J. Romberg, and T. Tao, "Robust uncertainty principles: exact signal reconstruction from highly incomplete frequency information," *IEEE Transactions on Information Theory*, vol. 52, no. 2, pp. 489–509, Feb. 2006.

[8] E. Candes and T. Tao, "The dantzig selector: Statistical estimation when p is much larger than n," *The Annals of Statistics*, vol. 35, no. 6, pp. 2313–2351, Dec. 2007.

[9] R. Tibshirani, "Regression shrinkage and selection via the lasso," *Journal of the Royal Statistical Society: Series B*, vol. 73, no. 3, pp. 273–282, 1996.

[10] Z. Yang and L. Xie, "On gridless sparse methods for line spectral estimation from complete and incomplete data," *IEEE Transactions on Signal Processing*, vol. 63, no. 12, pp. 3139–3153, June 2015.

[11] G. Tang, B. N. Bhaskar, P. Shah, and B. Recht, "Compressed sensing off the grid," *IEEE Transactions on Information Theory*, vol. 59, no. 11, pp. 7465–7490, Nov 2013.

[12] J. Tropp and A. Gilbert, "Signal recovery from random measurements via orthogonal matching pursuit," *IEEE Transactions on Information Theory*, vol. 53, no. 12, pp. 4650–4666, Dec. 2007.

[13] D. Needell and J. Tropp, "CoSAMP: Iterative signal recovery from incomplete and inaccurate samples," *Applied and Computational Harmonic Analysis*, vol. 26, no. 3, pp. 301 – 321, 2009.

[14] L. Potter, E. Ertin, J. Parker, and M. Cetin, "Sparsity and compressed sensing in radar imaging," *Proceedings of the IEEE*, vol. 98, no. 6, pp. 1006–1020, June 2010.

[15] K. Gedalyahu and Y. Eldar, "Time-delay estimation from low-rate samples: A union of subspaces approach," *IEEE Transactions on Signal Processing,*, vol. 58, no. 6, pp. 3017–3031, June 2010.

[16] C.-Y. Chen and P. Vaidyanathan, "Compressed sensing in mimo radar," in *Signals, Systems and Computers, 2008 42nd Asilomar Conference on*, Oct 2008, pp. 41–44.

[17] Y. Yu, A. Petropulu, and H. Poor, "Measurement matrix design for compressive sensing based mimo radar," *IEEE Transactions on Signal Processing*, vol. 59, no. 11, pp. 5338–5352, Nov. 2011.

[18] M. Herman and T. Strohmer, "High-resolution radar via compressed sensing," *IEEE Transactions on Signal Processing*, vol. 57, no. 6, pp. 2275–2284, June 2009.

[19] T. Strohmer and B. Friedlander, "Analysis of sparse MIMO radar," *Applied and Computational Harmonic Analysis*, vol. 37, no. 3, pp. 361 – 388, 2014.

[20] T. Strohmer and H. Wang, "Accurate imaging of moving targets via random sensor arrays and kerdock codes," *Inverse Problems*, vol. 29, no. 8, p. 085001, 2013.

[21] D. Dorsch and H. Rauhut, "Refined analysis of sparse MIMO radar," *CoRR*, vol. abs/1509.03625, 2015.

[22] M. Hügel, H. Rauhut, and T. Strohmer, " Remote sensing via ℓ_1-minimization," *Foundations of Computational Mathematics*, vol. 14, no. 1, pp. 115–150, 2014.

[23] Y. Yu, A. Petropulu, and H. Poor, "Cssf mimo radar: Compressive-sensing and step-frequency based mimo radar," *IEEE Transactions on Aerospace and Electronic Systems*, vol. 48, no. 2, pp. 1490–1504, APRIL 2012.

[24] B. Li and A. Petropulu, "Rip analysis of the measurement matrix for compressive sensing-based mimo radars," in *IEEE 8th Sensor Array and Multichannel Signal Processing Workshop (SAM), 2014*, June 2014, pp. 497–500.

[25] M. Shastry, R. Narayanan, and M. Rangaswamy, "Sparsity-based signal processing for noise radar

imaging," *IEEE Transactions on Aerospace and Electronic Systems*, vol. 51, no. 1, pp. 314–325, Jan. 2015.

[26] E. Baransky, G. Itzhak, N. Wagner, I. Shmuel, E. Shoshan, and Y. Eldar, "Sub-nyquist radar prototype: Hardware and algorithm," *IEEE Transactions on Aerospace and Electronic Systems,*, vol. 50, no. 2, pp. 809–822, Apr. 2014.

[27] O. Bar-Ilan and Y. C. Eldar, "Sub-nyquist radar via doppler focusing," *IEEE Transactions on Signal Processing*, vol. 62, no. 7, pp. 1796–1811, April 2014.

[28] M. Rossi, A. Haimovich, and Y. Eldar, "Spatial compressive sensing in mimo radar with random arrays," in *Information Sciences and Systems (CISS), 2012 46th Annual Conference on*, Mar. 2012, pp. 1–6.

[29] Y. Chi, "Sparse mimo radar via structured matrix completion," in *Global Conference on Signal and Information Processing (GlobalSIP), 2013 IEEE*, Dec 2013, pp. 321–324.

[30] S. Sun, W. Bajwa, and A. Petropulu, "Mimo-mc radar: A mimo radar approach based on matrix completion," *IEEE Transactions on Aerospace and Electronic Systems*, vol. 51, no. 3, pp. 1839–1852, July 2015.

[31] M. Duarte and R. Baraniuk, "Spectral compressive sensing," *Applied and Computational Harmonic Analysis*, vol. 35, no. 1, pp. 111 – 129, 2013.

[32] A. Gilbert, M. Strauss, and J. Tropp, "A tutorial on fast fourier sampling," *IEEE Signal Processing Magazine*, vol. 25, no. 2, pp. 57–66, Mar. 2008.

[33] E. Ertin, "Frequency diverse waveforms for compressive radar sensing," in *Waveform Diversity and Design Conference (WDD), 2010 International*, Aug. 2010, pp. 000 216–000 219.

[34] E. Ertin, L. Potter, and R. Moses, "Sparse target recovery performance of multi-frequency chirp waveforms," in *19th European Signal Processing Conference, 2011*, Aug 2011, pp. 446–450.

[35] T. T. Cai and T. Jiang, "Limiting laws of coherence of random matrices with applications to testing covariance structure and construction of compressed sensing matrices," *The Annals of Statistics*, vol. 39, no. 3, pp. 1496–1525, June 2011.

[36] E. Candes and Y. Plan, "Near-ideal model selection by l1 minimization," *The Annals of Statistics*, vol. 37, no. 5A, pp. 2145–2177, Oct. 2009.

[37] N. Sugavanam, "Compressive sampling in radar imaging," Ph. D. Dissertation. Ohio State University, 2017.

[38] W. Bajwa, "Geometry of random toeplitz-block sensing matrices: bounds and implications for sparse signal processing," *Proc. SPIE*, vol. 8365, pp. 836 505–836 505–7, 2012.

[39] N. Sugavanam and E. Ertin, "Recovery guarantees for MIMO radar using multi-frequency LFM waveform," in *2016 IEEE Radar Conference (RadarConf)*, May 2016, pp. 1–6.

[40] N. Sugavanam and E. Ertin "Recovery guarantees for multifrequency chirp waveforms in compressed radar sensing," *CoRR*, vol. abs/1508.07969, 2015.

[41] R. Baraniuk, M. Davenport, R. A. DeVore, and M. B. Wakin, "A simple proof of the restricted isometry property for random matrices," *Constructive Approximation*, vol. 28, no. 3, pp. 253–263, Dec. 2008.

[42] J. Haupt, W. Bajwa, G. Raz, and R. Nowak, "Toeplitz compressed sensing matrices with applications to sparse channel estimation," *IEEE Transactions on Information Theory*, vol. 56, no. 11, pp. 5862–5875, Nov. 2010.

[43] J. Romberg, "Compressive sensing by random convolution," *SIAM J. Img. Sci.*, vol. 2, no. 4, pp. 1098–1128, Nov. 2009.

[44] H. Rauhut, J. Romberg, and J. A. Tropp, "Restricted isometries for partial random circulant matrices," *Applied and Computational Harmonic Analysis*, vol. 32, no. 2, pp. 242 – 254, 2012.

[45] F. Krahmer, S. Mendelson, and H. Rauhut, "Suprema of chaos processes and the restricted isometry property," *Communications on Pure and Applied Mathematics*, vol. 67, no. 11, pp. 1877–1904, 2014.

[46] S. Foucart and H. Rauhut, *A Mathematical Introduction to Compressive Sensing*. Birkhouser, Basel, 2013.

[47] S. S. Chen, D. L. Donoho, and M. A. Saunders, "Atomic decomposition by basis pursuit," *SIAM Rev.*, vol. 43, no. 1, pp. 129–159, Jan. 2001.

[48] E. Candes, "The restricted isometry property and its implications for compressed sensing," *Comptes Rendus Mathematique*, vol. 346, no. 9-10, pp. 589–592, May 2008.

[49] N. Boyd, G. Schiebinger, and B. Recht, "The alternating descent conditional gradient method for sparse inverse problems," SIAM Journal on Optimization, vol. 27, no. 2, pp. 616–639, 2017.

[50] G. Tang, B. N. Bhaskar, and B. Recht, "Sparse recovery over continuous dictionaries -just discretize," in 2013 Asilomar Conference on Signals, Systems and Computers, Nov 2013, pp. 1043–1047.

[51] Z. Ben-Haim, Y. C. Eldar, and M. Elad, "Coherence-based performance guar- antees for estimating a sparse vector under random noise," IEEE Transactions on Signal Processing, vol. 58, no. 10, pp. 5030–5043, Oct 2010.

[52] Y. Chi, L. Scharf, A. Pezeshki, and A. Calderbank, "Sensitivity to basis mismatch in compressed sensing," IEEE Transactions on Signal Processing, vol. 59, no. 5, pp. 2182–2195, May 2011.

[53] V. Chandrasekaran, B. Recht, P. A. Parrilo, and A. S. Willsky, "The convex geometry of linear inverse problems," Foundations of Computational Mathe- matics,, vol. 12, no. 6, pp. 805–849, 2012